Epilepsy & Behavior 21 (2011) 407–411

Contents lists available at ScienceDirect

Epilepsy & Behavior

journal homepage: www.elsevier.com/locate/yebeh

Structural abnormalities of the thalamus in juvenile myoclonic epilepsy

Susana Barreto Mory [a], Luiz E. Betting [a,b,c,*], Paula T. Fernandes [a,b], Iscia Lopes-Cendes [d], Marilisa M. Guerreiro [a,b], Carlos A.M. Guerreiro [a,b], Fernando Cendes [a,b], Li M. Li [a,b]

[a] Department of Neurology, Faculty of Medical Sciences, University of Campinas (UNICAMP), Campinas, Brazil
[b] CInAPCe Program, Faculty of Medical Sciences, University of Campinas (UNICAMP), Campinas, Brazil
[c] Department of Neurology, Psychology and Psychiatry, Faculdade de Medicina de Botucatu, Universidade Estadual Paulista (UNESP), Sao Paulo, Brazil
[d] Department of Medical Genetics, Faculty of Medical Sciences, University of Campinas (UNICAMP), Campinas, Brazil

ARTICLE INFO

Article history:
Received 8 March 2011
Revised 12 May 2011
Accepted 14 May 2011
Available online 23 June 2011

Keywords:
Epilepsy
Neuroimaging
Juvenile myoclonic epilepsy
Magnetic resonance
Volumetry
Voxel-based morphometry

ABSTRACT

Studies have suggested that the thalamus is a key structure in the pathophysiology of juvenile myoclonic epilepsy. The objective of the present investigation was to examine the thalami of patients with juvenile myoclonic epilepsy using a combination of multiple structural neuroimaging modalities. The association between these techniques may reveal the mechanisms underlying juvenile myoclonic epilepsy and help to identify the neuroanatomical structures involved. Twenty-one patients with juvenile myoclonic epilepsy (13 women, mean age = 30 ± 9 years) and a control group of 20 healthy individuals (10 women, mean age = 31 ± 8 years) underwent MRI in a 2-T scanner. The volumetric three-dimensional sequence was used for structural investigation. Evaluation of the thalamus comprised voxel-based morphometry, automatic volumetry, and shape analysis. Comparisons were performed between patient and control groups. Voxel-based morphometry analysis identified areas of atrophy located in the anterior portion of the thalamus. Post hoc analysis of automatic volumetry did not reveal significant differences between the groups. Shape analysis disclosed differences between patients and controls in the anterior and inferior portions of the right thalamus and in the anterior portion of the left thalamus. The present investigation confirms that thalami of patients with juvenile myoclonic epilepsy are structurally abnormal with impairments located mainly in the anterior and inferior sections.

1. Introduction

Idiopathic generalized epilepsies (IGEs) are common and underdiagnosed disorders characterized by generalized tonic–clonic, absence, and myoclonic seizures. Seizure onset is age related, usually occurs during adolescence, and the neurological examination is normal. Juvenile myoclonic epilepsy (JME) is the most frequent subsyndrome of the IGEs [1]. Importantly, under appropriate diagnosis and treatment, the patients have a high rate of complete seizure control. Otherwise, the impact of frequent seizures in children and adolescents is harmful.

The electrophysiological hallmark of JME is generalized spike-and-wave (GSW) discharges with normal background [1,2]. Qualitative MRI is usually normal in these patients, and on the basis of electrophysiological characteristics, the thalamus has been hypothesized to play an important role in the pathophysiology of JME [3]. This was confirmed in experimental animal models that showed that the thalamus is essential for maintenance of rhythmic GSW discharges [4]. However, the actual role of and details about the participation of the thalamus in the epileptogenesis of JME are currently under investigation.

Quantitative MRI has allowed the identification of minor abnormalities in patients with JME, and these changes are observed mainly in the frontal cortex [5,6]. The thalamus has also been examined in neuroimaging studies, and the pattern of neuroanatomical involvement described in patients with JME is not consistent [6–9]. Magnetic resonance spectroscopy (MRS) has also identified biochemical abnormalities in the cerebral cortex and thalamus of patients with JME [10–12]. These techniques are noninvasive and may be useful in better comprehending epilepsy disorders. The objective of the present study was to examine the thalamus of patients with JME by combining multiple structural neuroimaging modalities.

2. Methods

2.1. Subjects

Patients were consecutively recruited from the outpatient epilepsy clinic of our institution. JME diagnosis was based on clinical and electroencephalographic criteria [1,2]. For this investigation, all patients had their clinical history detailed and their medical records reviewed. At least one person who previously observed a typical

* Corresponding author at: Departamento de Neurologia, Psiquiatria e Psicologia, Faculdade de Medicina de Botucatu - UNESP - Univ Estadual Paulista, Zip Code 18618-970, Botucatu, SP, Brazil. Tel.: +55 14 3811 6260; fax: +55 14 3815 5965.
E-mail address: betting@fmb.unesp.br (L.E. Betting).

1525-5050/$ – see front matter © 2011 Elsevier Inc. All rights reserved.
doi:10.1016/j.yebeh.2011.05.018

seizure was also interviewed to corroborate seizure semiology. Patients had at least one EEG that showed typical GSW discharges with normal background. The EEGs were performed using the 10–20 international system of electrode placement. All recordings were obtained in the interictal state without sleep deprivation and with photic stimulation as well as hyperventilation. Neurological examinations were normal in all patients.

2.2. Imaging

Magnetic resonance images were acquired with a 2-T (GE Elscint, Haifa, Israel) scanner. All patients and a control group of 20 volunteers (10 women, mean age = 31 ± 8 years, range: 22–52) underwent MRI. The control subjects were recruited from the local community. All participants signed an informed consent form, and the investigation was approved by the local ethics committee. Volumetric (three-dimensional) T1-weighted images with 1-mm isotropic voxels were acquired using a spoiled gradient echo sequence with flip angle = 35°, repetition time = 22 ms, echo time = 9 ms, matrix = 256 × 220, field of view = 23 × 25 cm, and 1-mm thick sagittal slices. These images were used for the structural investigation. Images were acquired in Digital Imaging and Communications in Medicine (DICOM) format and converted to ANALYZE using the software MRICRO [13].

2.3. Voxel-based morphometry

For voxel-based morphometry (VBM), images had been previously processed using SPM5 software (Wellcome Trust Centre for Neuroimaging, London, England; www.fil.ion.ucl.ac.uk) and VBM5 extension (http://dbm.neuro.uni-jena.de). Images were first submitted to a 12-parameter affine transformation and then to nonlinear warping. This registration process was performed using the International Consortium for Brain Mapping (ICBM) template and was followed by tissue classification in cerebrospinal fluid, gray matter, and white matter. VBM5 uses a unified segmentation approach that integrates image registration, MRI inhomogeneity bias correction, and tissue classification [14,15]. The final images have improved signal-to-noise ratio. Tissue priors were not used for the segmentation to reduce population-specific bias and to avoid circularity problems because the initial image registration does not require initial tissue segmentation and vice versa [15,16]. By application of the Hidden Markov Field model to the segmented images, uncorrected voxels that were unlikely to represent determined tissue were also removed. The final result was better tissue classification. Images were also modulated to preserve the amount of gray matter deformed in the normalization process. Finally, all images were smoothed using a 10-mm full-width at half maximum gaussian kernel. This final step reduced the variability of the gray matter segmented images and allowed comparisons between groups.

Statistical analysis was performed using a general linear model. Analysis of covariance was conducted with age, gender, and total intracranial volumes as covariates. For these analyses, an absolute threshold masking of 0.1 was included. Analyses were conducted by searching for areas of increased and decreased gray matter volumes by comparing patients and controls. Because the objective of this study was specifically to evaluate the thalamus, a region of interest (ROI) analysis was performed for each thalamus. The ROI used was a mask of the thalamus with 7500 voxels for each side and the same number of resels [17]. This mask was also used for automatic volumetry. The level of significance selected was $P<0.05$ corrected for multiple comparisons (false discovery rate).

2.4. Volumetry

The Individual Brain Atlases using the Statistical Parametric Mapping (IBASPM) toolbox was used for automatic volumetry of the thalamus and for total intracranial volume estimation. This software is an atlas-based method that uses spatial normalization and segmentation routines of SPM for volume acquisition [17]. Segmented and normalized images were automatically labeled based on the Atlas of Anatomical labeling (AAL). Thalamic volumes obtained were normalized according to total intracranial volume. Registration and labeling accuracy was checked and observed for all participants. The volumes of the patients were compared with those of the controls using analysis of variance. Statistical significance was set at $P<0.05$. Tukey's multiple comparison test was used for post hoc analysis among the subgroups.

2.5. Shape analysis

Volumetry is a method that cannot identify the exact point of structural abnormality. Furthermore, volumes may be equivalent and morphology may differ among structures. Shape analysis is a method that can help determine these differences and improve the visualization of structural abnormalities. For this investigation, we used thalami segmented by IBASPM. Shape analysis was conducted using parametric boundary descriptions (spherical harmonics, SPHARM) [18]. The segmented images were processed to correct small interior holes, and a minimal smooth operation was performed. Images were then converted to segmented meshes and submitted to spherical parameterization. SPHARM descriptors were computed from the mesh and its spherical parameterization. The SPHARM descriptors were analyzed and sampled into triangulated surfaces. Group analysis was performed using Hotelling's t^2 test, a multivariate version of Student's t test. Statistical and distance maps between the mean surfaces of the control and patients groups were provided to visualize the results [18].

3. Results

3.1. Demographics data

Twenty-one patients with JME (13 women, mean age = 30 ± 9, range: 20–50) were included in this study. Family history of epilepsy was present in 17 patients. Seven patients had myoclonic, absence, and generalized tonic–clonic seizures at the time of evaluation. The remainder of the patients had a combination of myoclonic and generalized tonic–clonic seizures. Mean age at seizure onset was 13 ± 8 years (range: 4–45). Mean time since last seizure was 4 ± 3 years (range: 1–12). Sixteen patients were being treated with valproate, three with carbamazepine, and two with phenobarbital.

3.2. Electroencephalography data

Seventy-nine EEGs were recorded (mean = 3.7 exams per patient, range: 1–9). Generalized discharges were observed in 45 exams (mean = 2.1 exams with generalized discharges per patient, range: 1–7). Focal abnormalities (defined as well-characterized focal sharp or slow waves and clear asymmetries of frequency and amplitude) were observed in 10 exams of four patients. Twenty-four EEGs were normal.

3.3. Structural findings

Qualitative analysis of the sequence used for this investigation was normal in all patients and controls. All three quantitative methods used indicated differences between patients with JME and controls.

Voxel-based morphometry ROI analysis identified areas of thalamic atrophy in the anterior portion the thalamus (coordinates: $x = -5, y = -10, z = -1$ and $x = 6, y = -9, z = -3$; cluster size: 153 for the left and 20 for the right thalamus; P value 0.017 and 0.034 false discovery rate corrected). Fig. 1 illustrates these results.

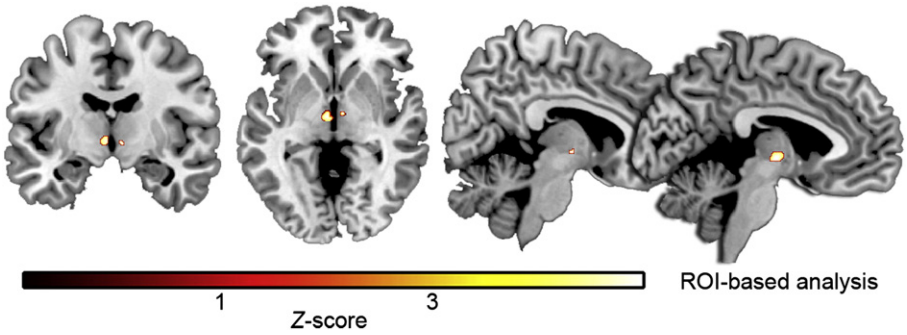

Fig. 1. Results of voxel-based morphometry analysis. The figure represents the statistical parametrical map of the region of interest comparisons between patients with JME and controls. Areas of gray matter atrophy are color coded, and the color scale at the bottom of the figure indicates the number of standard deviations relative to controls. The results are displayed in an anatomical template. The figures are presented in neurological convention (right on right).

Automatic volumetry showed differences in the left and right thalamic volumes of patients as compared with controls ($P = 0.03$). However, post hoc analysis did not detect differences in the subgroups. The mean normalized thalamic volumes of the patients were 4053 ± 375 mm^3 for the left thalamus and 4349 ± 380 mm^3 for the right thalamus. Mean normalized thalamic volumes of controls were 4097 ± 415 mm^3 for the left thalamus and 4270 ± 298 mm^3 for the right thalamus (Fig. 2).

Shape analysis revealed differences between patients with JME and controls in the anterior and inferior portions of the right thalamus and in the anterior portion of the left thalamus. Distance maps confirmed that these areas had major displacements as compared with the mean thalamic shapes of patients and controls (Fig. 3).

4. Discussion

The present investigation emphasizes the involvement of the thalamus in JME. Additional information regarding the participation of the thalamus in the mechanism of generalized seizures and JME was also provided. Our investigation demonstrates that thalamic atrophy is localized to the anterior and inferior portions of this structure. Anatomically, the nuclei in the anterior portion of the human thalamus have extensive connections with cortical structures. This integration is a key point in the pathophysiology of GSW discharges in IGEs [4].

Previous investigations have demonstrated thalamic atrophy in patients with IGEs. The reported regions of atrophy were not uniform and included the ventrolateral, ventromedial, and medial dorsal thalamus [8,9,19]. Intriguingly, previous analyses of patients with IGEs and absence seizures performed by our group identified increased anterior thalamic volumes [6,7]. Some investigators have failed to observe any thalamic abnormalities [20,21]. A possible explanation for these differences may be methodological differences in VBM. Indeed, there is considerable variability of the gray matter across different scanners observed in the thalamic nuclei [22], and previous studies have confirmed that the variation in this area is relatively large [23]. Another point is that all of these investigations were performed in different groups of patients. Our previous investigation was performed in patients with absence seizures. In the current investigation, only seven patients had absence seizures. These findings support the hypothesis of different mechanisms for generalized seizures. Thalamic anatomy may be modulated by other factors as well. Seizure frequency, antiepileptic drugs, and genetic profile may also influence the final arrangement of the thalamus. Therefore, current results suggest that thalamic morphology is associated with the subsyndrome and the predominant seizure type in patients with IGEs.

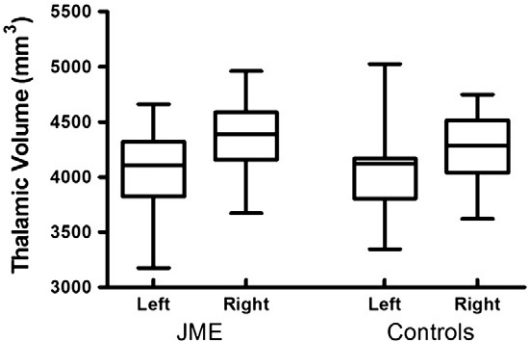

Fig. 2. Box-and-whisker plots of thalamic volumes for patient and control groups. Volumes are expressed in cubic millimeters (mm^3) and normalized according to total intracranial volume. JME, juvenile myoclonic epilepsy.

With the use of EEG–fMRI techniques, previous investigations have demonstrated significant thalamic activation in patients with IGEs [24,25]. Anterior, centromedian, and parafascicular thalamic nuclei were also activated during GSW discharges [26]. Additionally, these authors suggested that centromedian and parafascicular thalamic nuclei are involved in the maintenance of GSW discharges based on different time courses of activation [26]. Interestingly, the topography of the structural abnormality disclosed in this study is related to the centromedian–parafascicular complex identified in the EEG–fMRI findings.

White matter abnormalities have been described in a region related to the anterior thalamus and prefrontal cortex [27]. In this previous study, the authors used diffusion tensor imaging voxelwise analysis to compare 10 patients with JME with a control group. The observation of an atrophic anterior thalamus as described here may be related to the diffusion tensor imaging findings depicting the abnormal network of JME patients. The current methodology is not able to pinpoint the exact mechanism behind those areas of thalamic atrophy. However, there is evidence of increased interictal thalamic metabolism which is related to the amount of spike–wave activity [28]. This increased metabolism may be related to tissue damage and thalamic atrophy in patients with JME, especially those with generalized tonic–clonic seizures. This hypothesis is plausible as there are reports that thalamic volumes are correlated with the duration of epilepsy in JME, and in focal seizures the duration of epilepsy is also associated with the amount of gray matter loss [19,29]. Further neuroimaging investigations of patients with IGE with a more homogeneous clinical and electroencephalographic phenotype would be helpful in gaining an understanding of IGEs.

Our multimodal approach allowed us to detect a reduction in the volume of the thalamus in the anterior portions. The congruence of VBM and shape analysis makes our results credible. The reduction in *N*-acetyl aspartate described in MRS investigations probably is

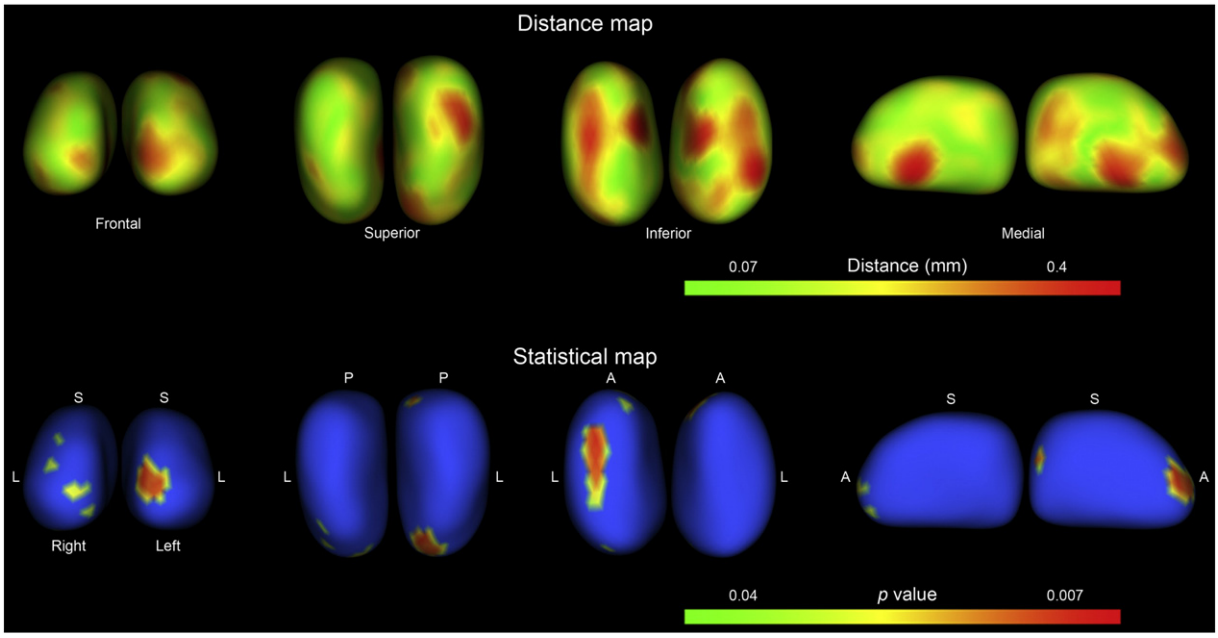

Fig. 3. Results of the shape analysis of thalami. The results are displayed in two maps. The distance map shows the distances in millimeters between the mean shapes of the right and left thalamus generated for patients and controls. The inferior row shows the statistical map of the comparison between the shapes of patients and controls. The maps are color coded according to the scale in the inferior portion of the figures. For both maps there are four pairs (right and left thalamus) of figures displayed in frontal, superior, inferior, and medial views. L, lateral; S, superior; P, posterior; A, anterior.

connected to these structural findings. Neuronal or axonal metabolic dysfunctions are possible explanations for the decreased concentration of *N*-acetyl aspartate. Therefore, the changes observed in thalamic morphology may be related to this abnormality [11,30].

The evidence available in the literature to date strongly supports a cortical origin of the GSW and seizure generation for JME [4,31]. However, although involvement of the thalamus occurs secondarily, its participation is essential in seizure pathogenesis. Again, it is difficult to conceive the exact underlying abnormalities behind the changes in thalamic shape and volume detected here. The interconnections between cortical areas and the thalamus are very extensive and several structures could be implicated. Furthermore, using EEG–fMRI one study clearly demonstrated important intersubject variability of activated areas, including the thalamus, in patients with absence epilepsy [31]. This evidence supports an association of varied mechanisms and networks with absence seizures. The impact of these findings in the thalamic structure remains to be established. Hence, this peculiarity may also be responsible for the divergence between the findings on thalamic volumes in patients with IGE.

One potential drawback of the current investigation is that the thalamic boundaries are subtle and 2-T MRI is not able to clearly differentiate the thalamic nuclei. With higher MRI field strength and new imaging techniques, this problem will probably be progressively reduced and the precise nuclei involved in the mechanisms of IGE may be determined. This recognition is important because it may open several opportunities for research which includes the fields of diagnosis, treatment, and genetic investigations.

Automatic segmentation and ROI-based VBM produce volumetric results comparable to those obtained with manual segmentation [32]. The automatic processing of the images implemented in these methods reduces the time of interaction with the machine and investigator bias. For this reason, these techniques are considered powerful tools for the detection of structural abnormalities in the brain. Shape analysis is another interesting method for investigating brain structures because of its ability to precisely locate morphological changes. Moreover, shape analysis can detect structural abnormalities that are not observed by conventional volumetry. The combination of all these neuroimaging techniques and modalities is important because they use different approaches, and therefore, the results may be cross-referenced. Thus, the comprehensive use of quantitative MRI is a crucial step in the investigation and understanding of the mechanisms behind epilepsies.

Conflict of interest statement

The authors have no conflicts of interest.

Acknowledgment

This study was supported by grants from the Fundação de Amparo à Pesquisa do Estado de São Paulo (FAPESP).

References

[1] Commission on Classification and Terminology of the International League Against Epilepsy. Proposal for revised classification of epilepsies and epileptic syndromes. Epilepsia 1989;30:389–99.
[2] Panayiotopoulos CP. Idiopathic generalized epilepsies. In: Panayiotopoulos CP, editor. A clinical guide to epileptic syndromes and their treatment. Oxfordshire: Bladon Medical; 2002. p. 115–60.
[3] Gloor P. Generalized cortico-reticular epilepsies: some considerations on the pathophysiology of generalized bilaterally synchronous spike and wave discharge. Epilepsia 1968;9:249–63.
[4] Meeren HK, Pijn JP, Van Luijtelaar EL, Coenen AML, Lopes da Silva FH. Cortical focus drives widespread corticothalamic networks during spontaneous absence seizures in rats. J Neurosci 2002;22:1480–95.
[5] Woermann FG, Free SL, Koepp MF, Sisodiya SM, Duncan JS. Abnormal cerebral structure in juvenile myoclonic epilepsy demonstrated with voxel-based analysis of MRI. Brain 1999;122:2101–7.
[6] Betting LE, Mory SB, Li LM, Lopes-Cendes I, Guerreiro MM, Guerreiro CA, et al. Voxel-based morphometry in patients with idiopathic generalized epilepsies. NeuroImage 2006;32:498–502.
[7] Betting LE, Mory SB, Lopes-Cendes I, Li LM, Guerreiro MM, Guerreiro CA, et al. MRI volumetry shows increased anterior thalamic volumes in patients with absence seizures. Epilepsy Behav 2006;8:575–80.
[8] Chan CH, Briellmann RS, Pell GS, Scheffer IE, Abbot DF, Jackson GD. Thalamic atrophy in childhood absence epilepsy. Epilepsia 2006;47:399–405.
[9] Helms G, Ciumas C, Kyaga S, Savic I. Increased thalamus levels of glutamate and glutamine (Glx) in patients with idiopathic generalised epilepsy. J Neurol Neurosurg Psychiatry 2006;77:489–94.

[10] Savic I, Lekvall A, Greitz D, Helms G. MR spectroscopy shows reduced frontal lobe concentrations of *N*-acetyl aspartate in patients with juvenile myoclonic epilepsy. Epilepsia 2000;41:290–6.
[11] Mory SB, Li LM, Guerreiro CAM, Cendes F. Thalamic dysfunction in juvenile myoclonic epilepsy: a proton MRS study. Epilepsia 2003;44:1402–5.
[12] Simister RJ, McLean MA, Barker GJ, Duncan JS. Proton MRS reveals frontal lobe metabolite abnormalities in idiopathic generalized epilepsy. Neurology 2003;61: 897–902.
[13] Rorden C, Brett M. Stereotaxic display of brain lesions. Behav Neurol 2000;12: 191–200.
[14] Ashburner J, Friston KJ. Unified segmentation. NeuroImage 2005;26:839–51.
[15] Meisenzahl EM, Koutsouleris N, Gaser C, et al. Structural brain alterations in subjects at high-risk of psychosis: a voxel-based morphometric study. Schizophr Res 2008;102:150–62.
[16] Good CD, Johnsrude IS, Ashburner J, Henson RN, Friston KJ, Frackowiak RS. A voxel-based morphometric study of ageing in 465 normal adult human brains. NeuroImage 2001;14:21–36.
[17] Aléman-Gómez Y, Melie-García L, Valdés-Hernandez P. IBASPM: toolbox for automatic parcellation of brain structures [CD]. In: Proceedings of the 12th Annual Meeting of the Organization for Human Brain Mapping, June 11–15, Florence, Italy. NeuroImage 2006;27:1.
[18] Zhao Z, Taylor WD, Styner M, Steffens DC, Krishnan KR, MacFall JR. Hippocampus shape analysis and late-life depression. PLoS ONE 2008;3:e1837.
[19] Kim JH, Lee JK, Koh SB, Lee SA, Lee JM, Kim SI, et al. Regional grey matter abnormalities in juvenile myoclonic epilepsy: a voxel-based morphometry study. NeuroImage 2007;37:1132–7.
[20] Natsume J, Bernasconi N, Andermann F, Bernasconi A. MRI volumetry of the thalamus in temporal, extratemporal, and idiopathic generalized epilepsy. Neurology 2003;60: 1296–300.
[21] Seeck M, Dreifuss S, Lantz G, Jallon P, Foletti G, Despland PA, et al. Subcortical nuclei volumetry in idiopathic generalized epilepsy. Epilepsia 2005;46: 1642–5.
[22] Stonnington CM, Tan G, Klöppel S, Chu C, Draganski B, Jack Jr CR, et al. Interpreting scan data acquired from multiple scanners: a study with Alzheimer's disease. NeuroImage 2008;39:1180–5.
[23] Pardoe H, Pell GS, Abbott DF, Berg AT, Jackson GD. Multi-site voxel-based morphometry: methods and a feasibility demonstration with childhood absence epilepsy. NeuroImage 2008;42:611–6.
[24] Aghakhani Y, Bagshaw AP, Bénar CG, Hawco C, Andermann F, Dubeau F, et al. fMRI activation during spike and wave discharges in idiopathic generalized epilepsy. Brain 2004;127:1127–44.
[25] Moeller F, Siebner HR, Wolff S, Muhle H, Boor R, Granert O, et al. Changes in activity of striato-thalamo-cortical network precede generalized spike wave discharges. NeuroImage 2008;39:1839–49.
[26] Tyvaert L, Chassagnon S, Sadikot A, LeVan P, Dubeau F, Gotman J. Thalamic nuclei activity in idiopathic generalized epilepsy: an EEG-fMRI study. Neurology 2009;73:2018–22.
[27] Deppe M, Kellinghaus C, Duning T, Möddel G, Mohammadi S, Deppe K, et al. Nerve fiber impairment of anterior thalamocortical circuitry in juvenile myoclonic epilepsy. Neurology 2008;71:1981–5.
[28] Kim JH, Im KC, Kim JS, Lee SA, Kang JK. Correlation of interictal spike–wave with thalamic glucose metabolism in juvenile myoclonic epilepsy. NeuroReport 2005;16:1151–5.
[29] Yasuda CL, Betting LE, Cendes F. Voxel-based morphometry and epilepsy. Expert Rev Neurother 2010;10:975–84.
[30] Bernasconi A, Bernasconi N, Natsume J, Antel SB, Andermann F, Arnold DL. Magnetic resonance spectroscopy and imaging of the thalamus in idiopathic generalized epilepsy. Brain 2003;126:2447–54.
[31] Moeller F, LeVan P, Muhle H, Stephani U, Dubeau F, Siniatchkin M, et al. Absence seizures: individual patterns revealed by EEG–fMRI. Epilepsia 2010;51:2000–10.
[32] Bergouignan L, Chupin M, Czechowska Y, Kinkingnéhun S, Lemogne C, Le Bastard G, et al. Can voxel based morphometry, manual segmentation and automated segmentation equally detect hippocampal volume differences in acute depression? NeuroImage 2009;45:29–37.